J. Fluid Mech. (1976), *vol.* 73, *part* 1, *pp.* 139–151
Printed in Great Britain

Linearized theory of axisymmetric hypersonic source flow past bodies of revolution

By M. YASUHARA, H. MITOME AND F. NAKAO
Department of Aeronautical Engineering, Nagoya University, Nagoya, Japan

(Received 18 March 1975)

The linearized theory of axisymmetric hypersonic source flow past a slender pointed body is treated by using linearized potential theory, assuming that the hypersonic parameter is less than unity. The governing equation in the transformed co-ordinates with the ratio of specific heats $\gamma = 1{\cdot}5$ shows a modified form relative to the equation for parallel flow, whereas that with $\gamma = 2$ shows essentially the same form. Some numerical calculations for a cone and a cone-cylinder are presented, and the surface pressure distributions obtained for both $\gamma = 1{\cdot}5$ and 2 show that there is a considerable pressure-distribution difference between source flow and parallel flow. The pressure on a cone in hypersonic source flow approaches zero downstream, while, if the cone has a cylindrical afterbody, the pressure recovers to the free-stream value quickly. This suggests that the static pressure probe for supersonic parallel flow is useful also in source flow.

1. Introduction

Effects of non-parallel flow towards a body are of current interest in external flows, as well as in internal flows. In practical cases of the flow past test bodies in hypersonic conical tunnels, or that in the central core of a free jet expanding into a vacuum (Ashkenas & Sherman 1966), the oncoming flow is essentially of source type. In some of these cases, the flow field significantly deviates from that with parallel oncoming flow, so that the perturbation theory starting from the parallel flow results becomes inadequate.

In hypersonic flows, most of the important problems require nonlinear treatments. Actually, in source flows, the Newtonian approximation or its modification can be conveniently used to obtain pressure distributions, as shown by Hall (1963), etc. Gorgui (1971) used the exact equations of motion to treat cones and wedges by expanding flow quantities in power series in the axial distance x from the nose divided by the source–nose distance r_N. Also, if the whole field is assumed to be supersonic, the method of characteristics can be applied (Krasnov 1970).

Furthermore, suppose the body is very slender, in the sense that the effective hypersonic parameter $\overline{\chi}$, the product of the free-stream Mach number M_0, and the angle ϵ of the body surface with respect to the free-stream direction (not the inclination angle of the body surface to the axial x direction), is smaller than

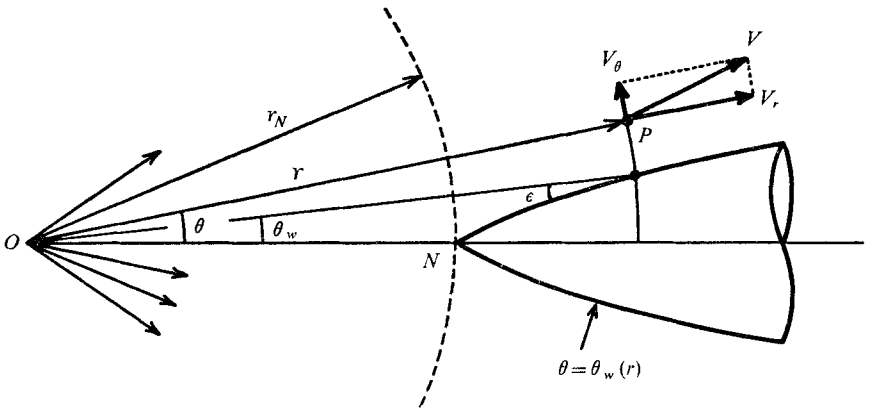

FIGURE 1. Flow geometry and co-ordinates.

unity. Then the flow field can be assumed to be isentropic with good accuracy, and the supersonic potential flow theory can be applied (Hayes & Probstein 1966; Van Dyke 1951). Further, a linearized analysis can be made if $\overline{\chi}$ is significantly smaller than unity.

The present paper treats the source flow past a very slender body with a linearized perturbation theory, and checks the possibility of the needle-type slender body for use as a static pressure probe in source flow. In practical cases, the hypersonic viscous interaction may cause strong entropy variation, especially around the nose. However, at the rear of the body, the interaction is estimated to be weak, so that the potential theory can give a good approximation.

2. Fundamental equations

Consider an axisymmetric hypersonic source flow past a pointed body of revolution, as shown in figure 1. If the polar co-ordinate system (r, θ) is used, the basic equations of the flow are

$$V_r \frac{\partial V_r}{\partial r} + \frac{V_\theta}{r}\frac{\partial V_r}{\partial \theta} - \frac{V_\theta^2}{r} = -\frac{1}{\rho}\frac{\partial p}{\partial r}, \tag{1}$$

$$V_r \frac{\partial V_\theta}{\partial r} + \frac{V_\theta}{r}\frac{\partial V_\theta}{\partial \theta} + \frac{V_r V_\theta}{r} = -\frac{1}{r\rho}\frac{\partial p}{\partial \theta}, \tag{2}$$

$$\frac{1}{r^2}\frac{\partial(\rho r^2 V_r)}{\partial r} + \frac{1}{r\sin\theta}\frac{\partial(\rho V_\theta \sin\theta)}{\partial \theta} = 0, \tag{3}$$

$$V_r \frac{\partial H}{\partial r} + \frac{V_\theta}{r}\frac{\partial H}{\partial \theta} = 0, \tag{4}$$

where

$$H \equiv \frac{\gamma}{\gamma - 1}\frac{p}{\rho} + \tfrac{1}{2}(V_r^2 + V_\theta^2).$$

In the above, V_r, V_θ, p, ρ and γ denote velocity components in the radial and azimuthal directions, the pressure, the density and the ratio of specific heats, respectively. In the present analysis, the flow Mach number is very large

compared with unity, and also the body is assumed to be slender in the sense that the hypersonic parameter $\bar{\chi} \equiv M_0 \epsilon$ is smaller than unity. This condition implies that θ in the disturbed flow field is very small everywhere. Because the flow is assumed to be isentropic, there exists a velocity potential Φ defined by

$$V_r = \frac{\partial \Phi}{\partial r} = \Phi_r, \quad V_\theta = \frac{1}{r}\frac{\partial \Phi}{\partial \theta} = \frac{1}{r}\Phi_\theta. \tag{5}$$

Then the gas-dynamic equation is derived from (1)–(5) as

$$\Phi_{rr}\left(1-\frac{\Phi_r^2}{a^2}\right)+\frac{\Phi_{\theta\theta}}{r^2}\left(1-\frac{\Phi_\theta^2}{r^2a^2}\right)-\frac{2\Phi_r\Phi_\theta\Phi_{\theta r}}{r^2a^2}+\frac{\Phi_r}{r}\left(2+\frac{\Phi_\theta^2}{r^2a^2}\right)+\frac{\Phi_\theta\cot\theta}{r^2}=0. \tag{6}$$

Here, the square a^2 of the local sound speed takes the form

$$(\gamma-1)(H-\tfrac{1}{2}\Phi_r^2-\tfrac{1}{2}r^{-2}\Phi_\theta^2),$$

with H constant. As usual in small disturbance theory, Φ is divided into free-stream and perturbation potentials ϕ_0 and ϕ_1 as

$$\Phi(r,\theta)=\phi_0(r)+\phi_1(r,\theta), \quad \Phi_r=\phi_{0r}+\phi_{1r}, \quad \Phi_\theta=\phi_{1\theta}. \tag{7}$$

Because the body is slender, and the perturbed velocity components are small compared with free radial velocity,

$$\phi_{0r} \gg \phi_{1r}, \phi_{1\theta}. \tag{8}$$

Then, after terms of higher order than $\Phi_\theta/(ra)$ (including $\Phi_\theta^2/(r^2a^2)$, $\Phi_r\Phi_\theta\Phi_{\theta r}/(r^2a^2)$, etc.) are neglected, (6) reduces to

$$(1-M_0^2)\phi_{0rr}+\frac{2}{r}\phi_{0r}=0, \tag{9}$$

$$(1-M_0^2)\phi_{1rr}+\frac{2M_0^2\{2+(\gamma-1)M_0^2\}}{r(1-M_0^2)}\phi_{1r}+\frac{\phi_{1\theta\theta}}{r^2}+\frac{2}{r}\phi_{1r}+\frac{\phi_{1\theta}}{\theta r^2}=0. \tag{10}$$

M_0 denotes the Mach number at point r in the free-source flow. Equation (9) gives the well-known solution for point-source flow, and M_0 is given as a function of r. Further, when $M_0 \gg 1$, M_0 can be approximated by

$$M_0/M_N \fallingdotseq (r/r_N)^{\gamma-1}. \tag{11}$$

The subscript N denotes the free-stream value at the nose of the body.

Suppose the non-dimensional variables s and ω, defined by

$$r/r_N \equiv s, \quad M_N\theta \equiv \omega, \tag{12}$$

are used as well as the approximation (11). Then the linearized perturbation equation for ϕ_1 becomes

$$s^{2\gamma}\left\{\phi_{1ss}+\frac{2(\gamma-1)}{s}\phi_{1s}\right\}=\phi_{1\omega\omega}+\frac{\phi_{1\omega}}{\omega}. \tag{13}$$

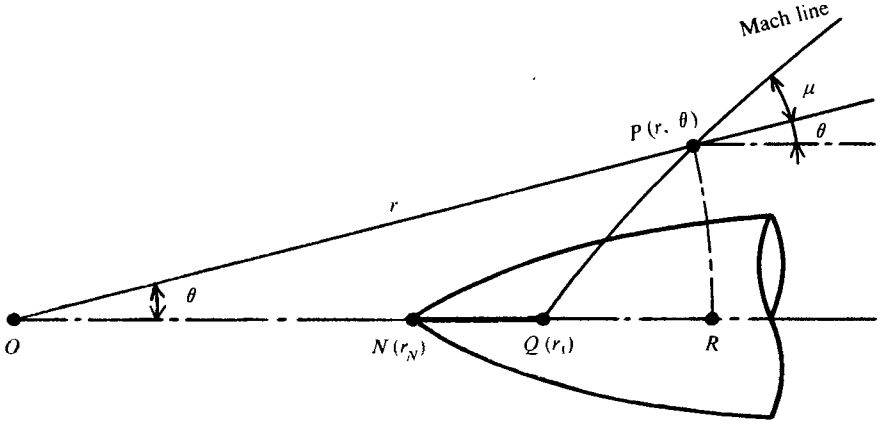

Figure 2. Region of influence of source line to point P.

Equation (13) is rather complicated to solve, but in the special cases when γ is equal to 1·5 or 2, it can be transformed to

$$\gamma = 1{\cdot}5, \qquad \phi_{1\zeta\zeta} + \frac{\phi_{1\zeta}}{\zeta} = \phi_{1\omega\omega} + \frac{\phi_{1\omega}}{\omega}, \quad \text{where} \quad \zeta \equiv 2/s^{\frac{1}{2}}, \tag{14a}$$

$$\gamma = 2, \qquad \phi_{1\xi\xi} = \phi_{1\omega\omega} + \frac{\phi_{1\omega}}{\omega}, \quad \text{where} \quad \xi \equiv \frac{1}{s}, \tag{14b}$$

respectively. Equation (14b) has the same form as the equation for the perturbation potential appearing in parallel flow past a body of revolution (Van Dyke 1951; Liepmann & Roshko 1957).

3. General solutions

The solutions of (14) can be obtained by using Green functions as

$$\gamma = 1{\cdot}5, \qquad \phi_1 = \int \frac{f(\zeta_1)\,d\zeta_1}{[\{(\zeta_1-\zeta)^2-\omega^2\}\{(\zeta_1+\zeta)^2-\omega^2\}]^{\frac{1}{2}}} = \int \frac{f(\zeta_1)\,d\zeta_1}{[\{\zeta_1^2-(\zeta^2+\omega^2)\}^2-(2\zeta\omega)^2]^{\frac{1}{2}}}, \tag{15a}$$

$$\gamma = 2, \qquad \phi_1 = \int \frac{g(\xi_1)\,d\xi_1}{[(\xi_1-\xi)^2-\omega^2]^{\frac{1}{2}}}. \tag{15b}$$

Here the unknown source distribution functions $f(\zeta_1)$ and $g(\xi_1)$ along the ζ and ξ axes can be determined from the boundary condition, and the limits of integration from physical considerations. As shown in figure 2, the part of the source line having influence on the point $P(r, \theta)$ lies between $N(r_N, 0)$ and $Q(r_1, 0)$, where μ is the Mach angle. The equation of the Mach line can be given by

$$r\frac{d\theta(r)}{dr} = s\frac{d\theta}{ds} = \mu \fallingdotseq \frac{1}{M_0} = \frac{1}{M_N s^{\gamma-1}}.$$

Integration of this from Q to P gives the relation between r_1 and (r, θ), from which N and Q are expressed in terms of the new variables as

$$\gamma = 1{\cdot}5, \qquad \zeta_1 = 2 \quad \text{at} \quad N, \qquad \zeta_1 = \zeta + \omega \quad \text{at} \quad Q,$$

$$\gamma = 2, \qquad \xi_1 = 1 \quad \text{at} \quad N, \qquad \xi_1 = \xi + \omega \quad \text{at} \quad Q.$$

As a result, the general solutions of (14) can be expressed as

$$\gamma = 1{\cdot}5, \qquad \phi_1 = \int_{\zeta+\omega}^{2} \frac{f(\zeta_1)\,d\zeta_1}{[\{\zeta_1^2-(\zeta^2+\omega^2)\}^2-(2\zeta\omega)^2]^{\frac{1}{2}}}, \tag{16a}$$

$$\gamma = 2, \qquad \phi_1 = \int_{\xi+\omega}^{1} \frac{g(\xi_1)\,d\xi_1}{[(\xi_1-\xi)^2-\omega^2]^{\frac{1}{2}}}. \tag{16b}$$

In order to avoid the singularity in the integrands at the lower limit of integration, the variables ζ_1 and ξ_1 are transformed into z and w, respectively, by

$$\gamma = 1{\cdot}5, \qquad \zeta_1^2 \equiv (\zeta^2+\omega^2)+2\zeta\omega\cosh z, \tag{17a}$$

$$\gamma = 2, \qquad \xi_1 \equiv \xi+\omega\cosh w. \tag{17b}$$

Further, if F is introduced by

$$f(\zeta_1)/2\zeta_1 \equiv F(\zeta_1^2), \tag{18}$$

then (16) can be reduced to

$$\gamma = 1{\cdot}5, \qquad \phi_1 = \int_0^{\cosh^{-1}\{[4-(\zeta^2+\omega^2)]/(2\zeta\omega)\}} F((\zeta^2+\omega^2)+2\zeta\omega\cosh z)\,dz, \tag{19a}$$

$$\gamma = 2, \qquad \phi_1 = \int_0^{\cosh^{-1}[(1-\xi)/\omega]} g(\xi+\omega\cosh w)\,dw. \tag{19b}$$

The boundary condition is that the flow is tangential to the body surface $\theta = \theta_w(r)$, i.e.

$$(V_\theta/V_r)_w = r\,d\theta_w/dr.$$

This condition can be expressed in the transformed variables as

$$\gamma = 1{\cdot}5, \qquad (\phi_{1\omega})_w = -\frac{2U_N r_N}{M_N^2}\frac{1}{\zeta}\frac{d\omega_w}{d\zeta}, \tag{20a}$$

$$\gamma = 2, \qquad (\phi_{1\omega})_w = -\frac{U_N r_N}{M_N^2}\frac{d\omega_w}{d\xi}. \tag{20b}$$

U_N is the velocity at the nose of the body.

The pressure coefficient referred to the free-stream nose pressure p_N is defined by

$$C_p = \frac{p_w-p_N}{\frac{1}{2}\rho_N U_N^2}$$

$$= \frac{2}{\gamma M_N^2}\left[\left\{1+\frac{\gamma-1}{2}M_N^2\left(1-\frac{V^2}{U_N^2}\right)\right\}^{\gamma/(\gamma-1)}-1\right]. \tag{21}$$

The perturbed pressure coefficient referred to the free-stream pressure p_0 is, within the linear approximation, expressed as

$$\frac{p_w-p_0}{\frac{1}{2}\rho_N U_N^2} = C_p - C_{p_0} \fallingdotseq -\frac{1}{s^2}\left\{2\frac{V_{1r}}{U_N}+\left(\frac{V_{1\theta}}{U_N}\right)^2\right\}.$$

If there is no body in the flow, the above value becomes zero, and this quantity can be regarded as the normalized perturbed pressure caused by the presence of a body.

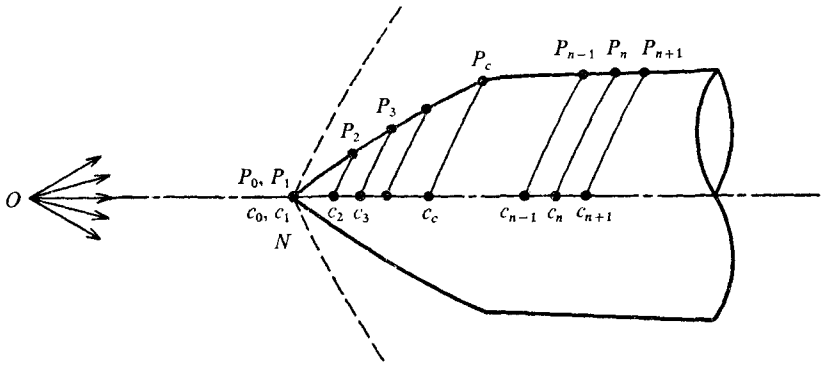

FIGURE 3. Method of solution for pointed body.

In the transformed co-ordinates, the above reduces to

$$\gamma = 1{\cdot}5, \quad C_p - C_{p0} \fallingdotseq -\frac{\zeta^4}{16}\left\{-\frac{\zeta^3}{4r_N}\frac{\phi_{1\zeta}}{U_N} + \left(\frac{M_N\zeta^2}{4r_N}\frac{\phi_{1\omega}}{U_N}\right)^2\right\}, \tag{22a}$$

$$\gamma = 2, \quad C_p - C_{p0} \fallingdotseq -\xi^2\left\{-\frac{2\xi^2}{r_N}\frac{\phi_{1\xi}}{U_N} + \left(\frac{M_N\xi}{r_N}\frac{\phi_{1\omega}}{U_N}\right)^2\right\}. \tag{22b}$$

C_{p0} denotes the pressure coefficient for free-source flow. In hypersonic free-source flow, the approximation

$$V_{0r}/U_N \fallingdotseq 1, \quad p_0/p_N \fallingdotseq s^{-2\gamma}$$

holds, from which C_{p0} can be expressed as

$$\gamma = 1{\cdot}5, \quad C_{p0} \fallingdotseq \frac{4}{3M_N^2}\left(\frac{1}{s^3} - 1\right) = \frac{4}{3M_N^2}\left(\frac{\zeta^6}{64} - 1\right). \tag{23a}$$

$$\gamma = 2, \quad C_{p0} \fallingdotseq \frac{1}{M_N^2}\left(\frac{1}{s^4} - 1\right) = \frac{1}{M_N^2}(\xi^4 - 1). \tag{23b}$$

4. Method of solution

In general, the solutions of (19) can be determined only numerically, and von Kármán & Moore's (1932) method is applied in the present analysis. The solutions are obtained by superposing a series of local solutions, in each of which the origin of the source distribution is chosen at c_n, as shown in figure 3, so that the solution is obtained as

$$\gamma = 1{\cdot}5, \quad \phi_1 = \sum_n (\phi_1)_n = \sum_n \int_0^{\cosh^{-1}\{[c_n^2 - (\zeta^2+\omega^2)]/(2\zeta\omega)\}} F_n((\zeta^2+\omega^2) + 2\zeta\omega\cosh z)\, dz, \tag{24a}$$

$$\gamma = 2, \quad \phi_1 = \sum_n (\phi_1)_n = \sum_n \int_0^{\cosh^{-1}[(c_n-\xi)/\omega]} g_n(\xi + \omega\cosh w)\, dw. \tag{24b}$$

$\zeta_1 = c_n$ and $\xi_1 = c_n$ denote each position of the origin of source distributions.

First, from the analogy with the potential for a cone in parallel flow, the source distribution functions are assumed to be

$$\gamma = 1{\cdot}5, \qquad F_n((\zeta^2+\omega^2)+2\zeta\omega\cosh z) = A_n(c_n^2-(\zeta^2+\omega^2+2\zeta\omega\cosh z)), \tag{25a}$$

$$\gamma = 2, \qquad g_n(\xi+\omega\cosh w) = B_n\{c_n-(\xi+\omega\cosh w)\}. \tag{25b}$$

A_n and B_n are unknown constants. In this case, with t_n and l_n defined by

$$\gamma = 1{\cdot}5, \qquad t_n(\zeta,\omega;c_n) \equiv \frac{2\zeta\omega}{c_n^2-(\zeta^2+\omega^2)}, \tag{26a}$$

$$\gamma = 2, \qquad l_n(\xi,\omega;c_n) \equiv \frac{\omega}{c_n-\xi}, \tag{26b}$$

ϕ_1 and its derivatives can be given as

$$\gamma = 1{\cdot}5, \qquad \left.\begin{aligned} \phi_{1n} &= A_n\{c_n^2-(\zeta^2+\omega^2)\}\{\operatorname{sech}^{-1}t_n-(1-t_n^2)^{\frac{1}{2}}\},\\ (\phi_{1n})_\zeta &= -2A_n\{\zeta\operatorname{sech}^{-1}t_n+\omega(1-t_n^2)^{\frac{1}{2}}/t_n\},\\ (\phi_{1n})_\omega &= -2A_n\{\omega\operatorname{sech}^{-1}t_n+\zeta(1-t_n^2)^{\frac{1}{2}}/t_n\}, \end{aligned}\right\} \tag{27a}$$

$$\gamma = 2, \qquad \left.\begin{aligned} \phi_{1n} &= B_n(c_n-\xi)\{\operatorname{sech}^{-1}l_n-(1-l_n^2)^{\frac{1}{2}}\},\\ (\phi_{1n})_\xi &= -B_n\operatorname{sech}^{-1}l_n,\\ (\phi_{1n})_\omega &= -B_n(1-l_n^2)^{\frac{1}{2}}/l_n. \end{aligned}\right\} \tag{27b}$$

The unknown constants A_n and B_n are determined such that the boundary condition is satisfied at the point P_{n+1}, i.e.

$$\gamma = 1{\cdot}5, \qquad \left[\sum_{i=0}^{n-1}(\phi_{1i})_\omega - 2A_n\{\omega\operatorname{sech}^{-1}t_n+\zeta(1-t_n^2)^{\frac{1}{2}}/t_n\}\right]_{P_{n+1}} = \left(-\frac{2U_N r_N}{M_N^2}\frac{1}{\zeta}\frac{d\omega_w}{d\zeta}\right)_{P_{n+1}}, \tag{28a}$$

$$\gamma = 2, \qquad \left[\sum_{i=0}^{n-1}(\phi_{1i})_\omega - B_n(1-l_n^2)^{\frac{1}{2}}/l_n\right]_{P_{n+1}} = \left(-\frac{U_N r_N}{M_N^2}\frac{d\omega_w}{d\xi}\right)_{P_{n+1}}. \tag{28b}$$

In order to begin the calculation, first a tangent cone to the body is assumed at the nose. The cone is expressed as

$$\omega_w = M_N\tan\alpha(1-\tfrac{1}{4}\zeta^2) = M_N\tan\alpha(1-\xi). \tag{29}$$

α corresponds to the semi-vertex angle of the body at the nose. Then, values of t_0 and l_0 at the nose, and also A_0 and B_0 are expressed explicitly as

$$\left.\begin{aligned} &\gamma = 1{\cdot}5, \qquad (t_0)_N = M_N\tan\alpha, \quad A_0 = -\frac{U_N r_N\tan^2\alpha}{4(1-M_N^2\tan^2\alpha)^{\frac{1}{2}}},\\ &\gamma = 2, \qquad (l_0)_N = M_N\tan\alpha, \quad B_0 = -\frac{U_N r_N\tan^2\alpha}{(1-M_N^2\tan^2\alpha)^{\frac{1}{2}}}. \end{aligned}\right\} \tag{30}$$

Using these constants, $(\phi_1)_0$ and its derivatives are calculated along the body surface. If this solution does not satisfy the boundary condition at P_2, then another source distribution with constant A_1 or B_1 is imposed from the nose with origin c_1. These constants A_1 and B_1 are determined such that the boundary

condition is satisfied at point P_2 using relations (28) above. After $\sum_{i=0}^{1}(\phi_1)_i$ have been caluclated on the surface of the body, a source distribution with origin c_2 is imposed and its constant is determined from the boundary condition at P_3. Then $\sum_{i=0}^{2}(\phi_1)_i$ can be calculated on the surface. This procedure is continued until every surface point satisfies the boundary condition.

If the body has a discontinuity in curvature like a cone-cylinder, the procedure just described above gives poor accuracy behind the corner, unless the intervals are chosen extremely small. According to Van Dyke (1951), however, the corner can be effectively removed by adding, with origin at c_c, the 'corner solution'. Analogously to Van Dyke's method, the source distribution functions at the corner are assumed to be

$$\gamma = 1{\cdot}5, \quad F_c(\zeta^2+\omega^2+2\zeta\omega\cosh z) = A_c[c_c^2-(\zeta^2+\omega^2+2\zeta\omega\cosh z)]^{\frac{1}{2}}, \tag{31a}$$

$$\gamma = 2, \quad g_c(\xi+\omega\cosh w) = B_c[c_c-(\xi+\omega\cosh w)]^{\frac{1}{2}}. \tag{31b}$$

A_c and B_c are unknown constants. In the above case, ϕ_{1c} and its derivatives can be obtained as

$$\gamma = 1{\cdot}5, \quad \left\{\begin{aligned} &\phi_{1c} = 2A_c(1+t_c)^{\frac{1}{2}}[c_c^2-(\zeta^2+\omega^2)]^{\frac{1}{2}}\{K(k)-E(k)\},\\ &(\phi_{1c})_\zeta = -\frac{2A_c}{[c_c^2-(\zeta^2+\omega^2)]^{\frac{1}{2}}(1+t_c)^{\frac{1}{2}}}\left\{(\zeta-\omega)K(k)+\frac{2\omega}{1-k^2}E(k)\right\},\\ &(\phi_{1c})_\omega = -\frac{2A_c}{[c_c^2-(\zeta^2+\omega^2)]^{\frac{1}{2}}(1+t_c)^{\frac{1}{2}}}\left\{(\omega-\zeta)K(k)+\frac{2\zeta}{1-k^2}E(k)\right\}, \end{aligned}\right. \tag{32a}$$

$$\gamma = 2, \quad \left\{\begin{aligned} &\phi_{1c} = \frac{4B_c}{\pi}(1-\xi)\left[\frac{\omega_{w,c}}{\omega}\right]^{\frac{1}{2}}(1+l_c)^{\frac{1}{2}}\left[\frac{2l_c}{1+l_c}\right]^{\frac{1}{2}}\{K(k)-E(k)\},\\ &(\phi_{1c})_\xi = -\frac{2B_c}{\pi}\left[\frac{\omega_{w,c}}{\omega}\right]^{\frac{1}{2}}\left[\frac{2l_c}{1+l_c}\right]^{\frac{1}{2}}K(k),\\ &(\phi_{1c})_\omega = -\frac{2B_c}{\pi}\left[\frac{\omega_{w,c}}{\omega}\right]^{\frac{1}{2}}\left[\frac{2l_c}{1+l_c}\right]^{\frac{1}{2}}\left(\frac{1+l_c}{l_c}E(k)-K(k)\right). \end{aligned}\right. \tag{32b}$$

Here

$$\gamma = 1{\cdot}5, \quad t_c \equiv \frac{2\zeta\omega}{c_c^2-(\zeta^2+\omega^2)}, \quad k^2 = \frac{1-t_c}{1+t_c}, \tag{33a}$$

$$\gamma = 2, \quad l_c \equiv \frac{\omega}{c_c-\xi}, \quad k^2 = \frac{1-l_c}{1+l_c}. \tag{33b}$$

K and E are the complete elliptic integrals of the first and second kind, with modulus k. The unknown constants A_c and B_c are determined from the condition that the flow is tangential to the body surface just behind the corner, i.e.

$$\gamma = 1{\cdot}5, \quad A_c = \frac{4r_N U_N}{\pi M_N^2 \zeta_c}\frac{(\zeta_c\omega_c)^{\frac{1}{2}}}{(\zeta_c+\omega_c)}\left(\frac{d(\omega_w)_b}{d\zeta}-\frac{d(\omega_w)_a}{d\zeta}\right), \tag{34a}$$

$$\gamma = 2, \quad B_c = \frac{r_N U_N}{M_N^2}\left(\frac{d(\omega_w)_b}{d\xi}-\frac{d(\omega_w)_a}{d\xi}\right). \tag{34b}$$

$(\omega_w)_a$ and $(\omega_w)_b$ correspond to the body shapes just ahead of and behind the corner, respectively.

5. Calculations and results for cone and cone-cylinder

As practical examples, the source flow past a cone and a cone-cylinder are analysed by the present method. The equations of the body surfaces in (ζ, ω) and (ξ, ω) variables are expressed as follows.

Cone,
$$\omega_w = M_N \tan\alpha(1-\tfrac{1}{4}\zeta^2) = M_N \tan\alpha(1-\xi). \tag{35}$$

Cone-cylinder,
$$\left.\begin{aligned} \omega_w &= \begin{cases} M_N \tan\alpha(1-\tfrac{1}{4}\zeta^2) & \text{for} \quad 2 \geqslant \zeta \geqslant \zeta_c, \\ M_N \tan\alpha(1-\xi) & \text{for} \quad 1 \geqslant \xi \geqslant \xi_c, \end{cases} \\ \omega_w &= \begin{cases} (M_N d/8r_N)\zeta^2 & \text{for} \quad \zeta_c \geqslant \zeta > 0, \\ (M_N d/2r_N)\xi & \text{for} \quad \xi_c \geqslant \xi > 0. \end{cases} \end{aligned}\right\} \tag{36}$$

α is the semi-vertex angle of the cone, and d is the diameter of the cylinder, as shown in figure 4.

In the case $\gamma = 2$, there exists a closed-form solution for cones, which can be expressed as

$$\left.\begin{aligned} \phi_1 &= B_0(1-\xi)\left\{\operatorname{sech}^{-1}\frac{\omega}{1-\xi} - \left[1-\left(\frac{\omega}{1-\xi}\right)^2\right]^{\frac{1}{2}}\right\}, \\ (\phi_{1\xi})_w &= \frac{U_N r_N \tan^2\alpha}{(1-M_N^2\tan^2\alpha)^{\frac{1}{2}}} \operatorname{sech}^{-1}(M_N \tan\alpha), \\ (\phi_{1\omega})_w &= \frac{U_N r_N \tan\alpha}{M_N}. \end{aligned}\right\} \tag{37}$$

This stems from the formal correspondence of the equation to that of parallel flow. On the other hand, there exists no such closed-form solution for the case $\gamma = 1{\cdot}5$, because the correspondence to the parallel flow is not perfect. Therefore, the step-by-step superposition explained in § 4 must be applied here.

For computations, the following numerical values are used: Mach number at the nose, $M_N = 7{\cdot}5$; semi-vertex angle of the cone, $\alpha = 4°$; diameter of the cylinder d divided by r_N, $d/r_N = 4/344 = 0{\cdot}0116$; hypersonic parameter at the nose, $\chi = M_N \tan\alpha = 0{\cdot}52$. It must be noted that the hypersonic parameter $\bar{\chi}$ at the nose takes the maximum value for cones and cone-cylinders, which is easily verified from the definition.

Conical part,
$$\theta_w \fallingdotseq \tan\alpha(1-s^{-1}),$$
$$\bar{\chi} \equiv M_0\epsilon = M_0(\alpha-\theta_w) \fallingdotseq (M_N s^{\gamma-1})(s^{-1}\tan\alpha) = M_N s^{-(2-\gamma)}\tan\alpha. \tag{38}$$

Cylindrical part,
$$\theta_w \fallingdotseq \frac{d}{2r_N}s^{-1},$$
$$\bar{\chi} \equiv M_0\epsilon = M_0\theta_w \fallingdotseq (M_N s^{\gamma-1})\left(\frac{d}{2r_N}s^{-1}\right) = M_N\frac{d}{2r_N}s^{-(2-\gamma)}. \tag{39}$$

From these relations, it is seen that, if $\gamma \leqslant 2$, the hypersonic parameter $\bar{\chi}$ takes the maximum value $M_N \tan\alpha$ at $s = 1$ (i.e. at the nose), and it remains constant ($\gamma = 2$) or decreases ($\gamma = 1{\cdot}5$) as s increases.

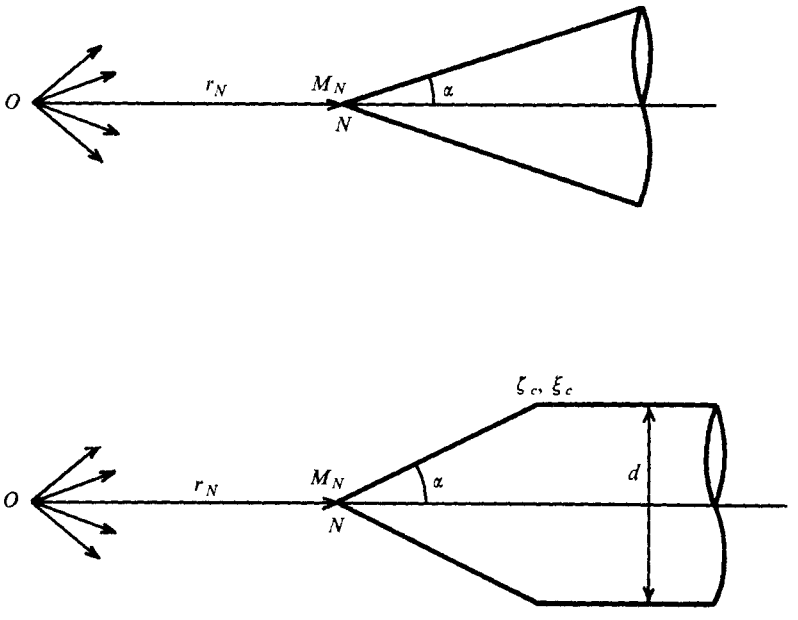

FIGURE 4. Dimension of bodies to be calculated.

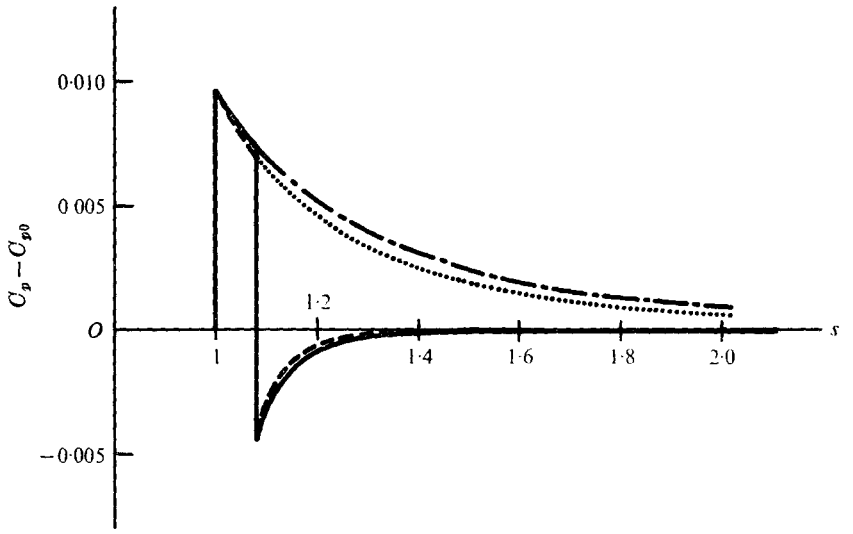

FIGURE 5. Distributions of the perturbed pressure coefficient $C_p - C_{p0}$. — · —, cone, $\gamma = 1{\cdot}5$; ·····, cone, $\gamma = 2$; ——, cone-cylinder, $\gamma = 1{\cdot}5$; – – –, cone-cylinder, $\gamma = 2$.

Results are shown in figures 5–7. Figure 5 shows the perturbed pressure coefficient $C_p - C_{p0}$ for both the cone and the cone-cylinder against dimensionless distance $s = r/r_N$. It is well known that, if the cone is in a parallel flow, the conical solution shows that the surface pressure is kept constant, while the present figure shows that, although the surface pressure at the nose takes the same value as that in a parallel flow, it decreases as s increases, approaching the free-stream

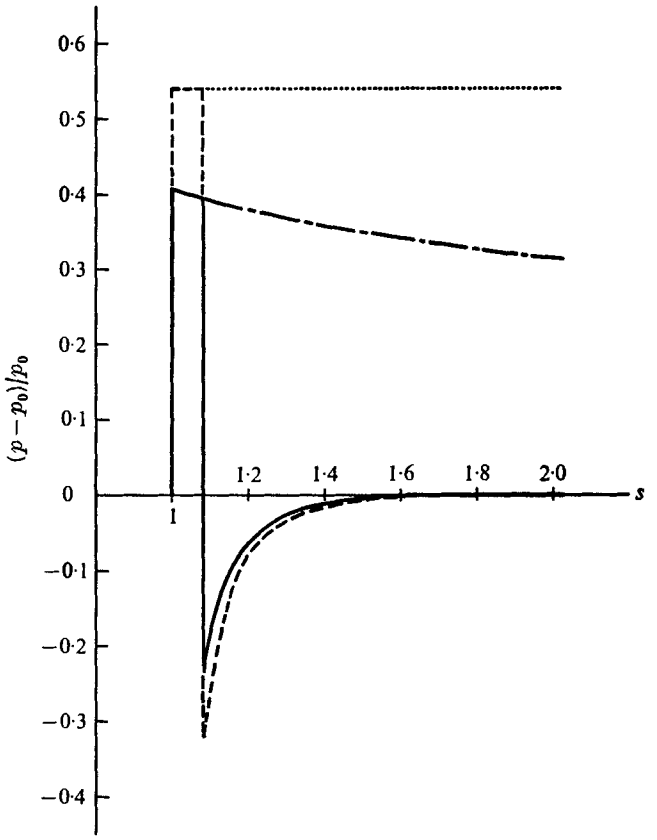

FIGURE 6. Difference between surface pressure p and free-stream value p_0 divided by p_0. — · —, cone, $\gamma = 1{\cdot}5$; ·····, cone, $\gamma = 2$; ——, cone-cylinder, $\gamma = 1{\cdot}5$; – – – –, cone-cylinder, $\gamma = 2$.

value. Also, the figure shows that the pressure for $\gamma = 1{\cdot}5$ takes a value a little higher than that for $\gamma = 2$. The term $C_p - C_{p0}$ gives the difference between the surface pressure coefficient and the free-stream one. The pressure distribution along the cone-cylinder shows a discontinuous pressure drop behind the corner point below the free-source flow value, then it approaches the free-stream value more quickly than the cone does. Exactly speaking, $(p-p_0)/p_0$ indicates the recovery of the surface pressure to the free-stream value. If this were very small compared with unity, then p could be used as an approximation to the free-stream pressure p_0. In figure 6, $(p-p_0)/p_0$ is plotted against s for the cone and the cone-cylinder in the present calculated cases. The figure shows that its value remains constant for the cone with $\gamma = 2$. This comes from the relations

$$C_p - C_{p0} = s^{-4}\tan^2\alpha\left(\frac{2\,\mathrm{sech}^{-1}(M_N\tan\alpha)}{(1-M_N^2\tan^2\alpha)^{\frac{1}{2}}} - 1\right), \tag{40}$$

$$C_{p0} = M_N^{-2}(s^{-4}-1), \tag{41}$$

$$\frac{p-p_0}{p_0} = M_N^2\tan^2\alpha\left(\frac{2\,\mathrm{sech}^{-1}(M_N\tan\alpha)}{(1-M_N^2\tan^2\alpha)^{\frac{1}{2}}} - 1\right). \tag{42}$$

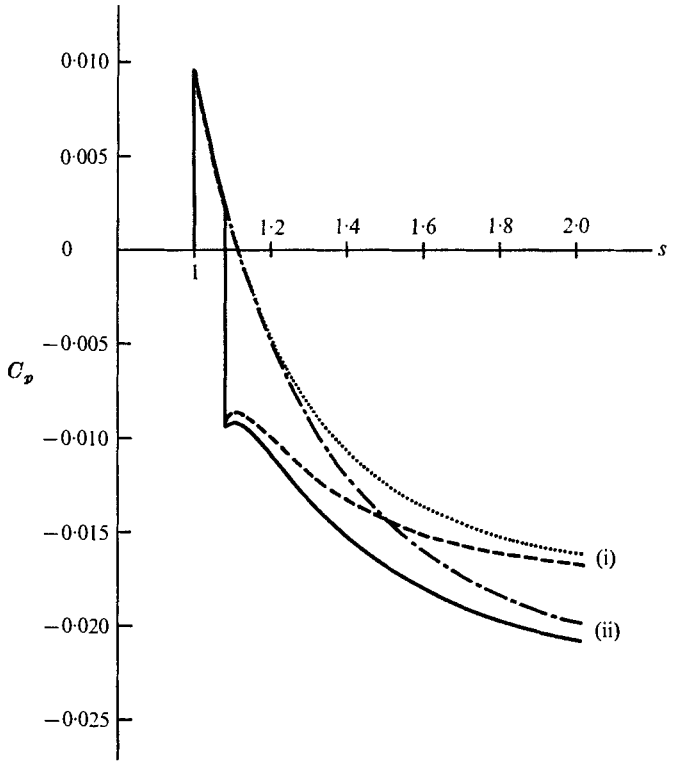

FIGURE 7. Distributions of the pressure coefficient C_p. (i) $s = \infty, \gamma = 2$; (ii) $s = \infty, \gamma = 1{\cdot}5$. —·—, cone, $\gamma = 1{\cdot}5$; ·····, cone, $\gamma = 2$; ——, cone-cylinder, $\gamma = 1{\cdot}5$; – – – –, cone-cylinder, $\gamma = 2$.

As is seen from (42), when $\gamma = 2$, $(p-p_0)/p_0$ in the linearized theory does not depend on s and keeps a constant value. For the cone with $\gamma = 1{\cdot}5$, $(p-p_0)/p_0$ decreases slightly as s increases. On the other hand, for the cone-cylinder, the value of $(p-p_0)/p_0$ behind the corner quickly approaches zero, which means that the surface pressure p there can be used as substitute for p_0. This fact suggests the possibility of using the needle type cone-cylinder as a static pressure probe in a source flow. It should be noted that the viscous effect, especially near the nose of the body, will cause interaction with the outer inviscid flow, and therefore the present results must be modified to include these effects. However, the pressure far downstream from the nose, where the interaction is weak, could be given by the present results with a good approximation.

Figure 7 shows the pressure coefficient C_p for both the cone and the cone-cylinder. As shown in figure 5, C_p approaches to C_{p0} as s increases, while C_{p0} approaches $-0{\cdot}0237$ for $\gamma = 1{\cdot}5$ and $-0{\cdot}0178$ for $\gamma = 2$. This is the reason why C_p for $\gamma = 1{\cdot}5$ and 2 in figure 7 approach different limits as s increases.

6. Conclusion

The theory for a slender pointed body with zero attack angle in a hypersonic source flow was treated by using inviscid linearized potential theory, assuming that the hypersonic parameter is significantly smaller than unity. The governing equation for hypersonic source flow with $\gamma = 1{\cdot}5$ shows a modified form relative to the equation for parallel flow in the transformed co-ordinate system, whereas that with $\gamma = 2$ shows essentially the same form as the equation for parallel flow. Some numerical calculations for a cone and a cone-cylinder were presented, and the obtained surface pressure distributions were shown for both $\gamma = 1{\cdot}5$ and 2. The computations demonstrate that the pressure coefficient on a cone in source flow decreases markedly downstream and approaches the free-stream value, whereas in parallel flow the pressure coefficient should remain constant. The difference between the surface pressure on a cone-cylinder p and the free-stream value p_0 divided by p_0 approaches zero behind the corner, which means that the surface pressure p there can be used as substitute for p_0. Thus, it may be suggested that the static pressure probe for supersonic parallel flow is useful even in source flow within the first approximation, provided that the hypersonic interaction parameter $\bar{\chi}$ is significantly smaller than unity, and also that the static pressure hole must be located reasonably far downstream.

The present theory is an extension of the supersonic linearized theory to hypersonic source flow, and it is assumed that the hypersonic parameter is significantly smaller than unity. In reality, the flow is also affected by viscosity, which, however, is not treated here.

The present work was partly supported by the scientific funds of the Ministry of Education, and some of the numerical computations were performed by FACOM 230-60 at the Computation Center, Nagoya University.

REFERENCES

ASHKENAS, H. & SHERMAN, F. S. 1966 *Rarefied Gas Dynamics Suppl.* **2** (3), 84.
GORGUI, M. A. 1971 *Aero. Quart.* **22**, 327.
HALL, J. G. 1963 *Cornell Aero. Lab. Rep. CAL* 128.
HAYES, W. D. & PROBSTEIN, R. F. 1966 *Hypersonic Flow Theory.* Academic.
KÁRMÁN, T. VON & MOORE, N. B. 1932 *Trans. A.S.M.E.* **54**, 303.
KRASNOV, N. F. 1970 *Aerodynamics of Bodies of Revolution.* American Elsevier.
LIEPMANN, H. W. & ROSHKO, A. 1957 *Elements of Gasdynamics.* Wiley.
VAN DYKE, M. D. 1951 *J. Aero. Sci.* **18**, 161.